Theoretical Study of Free-Radical-Mediated 5-*exo*-Trig Cyclizations of Chiral 3-Substituted Hepta-1,6-dienes

Philippe d'Antuono,[†] Alain Fritsch,[‡] Laurent Ducasse,[‡] Frédéric Castet,*[,‡] Philippe James,[§] and Yannick Landais[§]

Laboratoire de Chimie Théorique Appliquée, Facultés Universitaires Notre-Dame de la Paix, 61 rue de Bruxelles, B-5000 Namur, Belgium, Laboratoire de Physico-Chimie Moléculaire (UMR 5803, CNRS), Université Bordeaux I, 351, Cours de la Libération, 33405 Talence Cedex, France, and Laboratoire de Chimie Organique et Organométallique (UMR 5802, CNRS), Université Bordeaux I, 351, Cours de la Libération, 33405 Talence Cedex, France

Received: September 1, 2005; In Final Form: January 11, 2006

Free radical-mediated 5-*exo*-trig cyclizations of hepta-1,6-dienes incorporating allylsilane, alkyl and alkoxy analogues are modeled using correlated ab initio calculations. The structural, electronic and thermochemical properties of reactants, products and transition species involved in the key step of the radical cyclization process are analyzed and compared with those predicted by the Beckwith−Houk transition models. The product ratios are calculated from the Gibbs energy differences between the possible transition structures following the Curtin−Hammet principle and compared to experimental values.

1. Introduction

In a recent work,[1] James et al. studied the stereochemistry of free radical mediated 5-*exo*-trig cyclizations incorporating different substituents in the allylic position such as allylsilane ($SiMe_2Ph$) (i.e., **1a**), alkyl (*t*-Bu, Me) (i.e., **1b**) or alkoxy groups (OH, OTBS, $OCOCF_3$) (i.e., **3**) (Scheme 1). In particular, their study points out remarkable differences in the 1,2- and 1,5-stereocontrol with respect to the nature of the allylic substituent. Cyclization processes incorporating an allylsilane moiety are shown to provide the most efficient stereocontrol, leading to a single diastereomer of trisubstituted cyclopentane having a trans−cis stereochemistry (i.e., **2a**) with an excellent yield. A similar stereochemistry and an even better level of stereocontrol (obtained at 80 °C) are observed by introducing a *t*-Bu group in allylic position (**2b**). On the other hand, the corresponding process carried out with precursors having a methyl group in allylic position leads to a very low level of stereocontrol and to a mixture of the four possible cyclized stereomers. Finally, reactions incorporating allylic oxygenated groups (as in **3a**,**b**) give rise to the complementary selectivity of that observed with silicon, leading predominantly to the cis−cis isomer **4a**,**b**.

The stereochemical course of the 5-*exo*-trig cyclizations is qualitatively rationalized by the authors in terms of Beckwith−Houk transition state models. The combination of the steric and electronic effects of the SiR_3 group is thus assumed to decrease the number of reactive conformations at the cyclization transition states and to stabilize a partial positive charge at the radical center, thus inducing the very high level of stereocontrol. The complementary stereochemistry encountered with alkoxy substituents is assumed to be related to the electronic effects of oxygen, which are opposite to that of silicon. Moreover, a hydrogen bonding between the alcohol function in **3a** and the closest sulfonyl group would presumably stabilize the all-cis stereochemistry and the axial position adopted by the OH group. However, as mentioned by the authors, the better stereocontrol observed when R = $OCOCF_3$ and R = $OSiMe_2$-*t*-Bu (**3b**), in which hydrogen bonding cannot occur, seems to contradict this hypothesis.

SCHEME 1: Free-Radical 5-*exo*-Trig Cyclization of Chiral Hepta-1,6-dienes

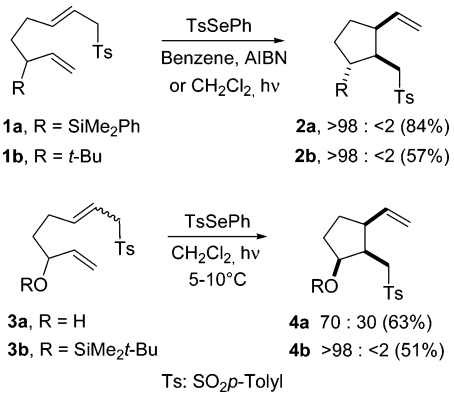

Therefore, the nature of the leading effects (steric and/or electronic) governing the stereochemistry of the 5-*exo*-trig cyclizations, and more specifically the very high 1,5- stereocontrol observed in the silicon series, are not clearly established. To provide some insights into the origin of the stereocontrol in these processes, we present here a series of high level ab initio calculations carried out on radical precursors incorporating the Si, *t*-Bu and OH groups. To reduce the computational costs, the key step of the cyclization process has been modeled by using simplified precursors (Scheme 2).

The sulfonyl group (Ts: SO_2-*p*-Tol) has been first removed and replaced in the calculations by a simple hydrogen atom. Despite interactions between the sulfonyl group and the allylic substituent that could constitute a non-negligible factor con-

* Corresponding author. E-mail: f.castet@lpcm.u-bordeaux1.fr.
[†] Facultés Universitaires Notre-Dame de la Paix.
[‡] Laboratoire de Physico-Chimie Moléculaire (UMR 5803, CNRS), Université Bordeaux I.
[§] Laboratoire de Chimie Organique et Organométallique (UMR 5802, CNRS), Université Bordeaux I.

10.1021/jp0549531 CCC: $33.50
Published on Web 02/18/2006

SCHEME 2: Three Steps of the Cyclization Process: (I) Reactive Form, (II) Transition State, (III) Cyclized Product (X = $SiMe_3$, *t*-Bu, OH)

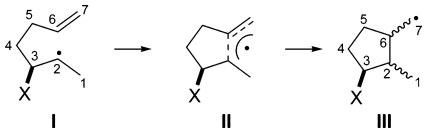

tributing to the level of stereocontrol, this first theoretical study mainly focused on the differences introduced in the electronic structure of radicals, in particular in their transition states, when varying the nature of the allylic group. In the silylated precursor, the $SiMe_2Ph$ group (as in **1a**, Scheme 1) was replaced by $SiMe_3$, because one can reasonably assume that the phenyl group has no direct influence on the cyclization process. Finally, solvent effects have not been accounted for, as it was demonstrated by James et al. that their impact on the observed stereoselectivities was not significant.[1]

All stationnary points, e.g., reactive, cyclized and transition species involved in the cyclization processes incorporating the various β-substituents were calculated and fully analyzed in terms of structural and electronic parameters. Quantum chemical results are checked against the structural hypotheses that have driven the synthesis, as well as against structures predicted by the Beckwith−Houk model.[2,3] Finally, the product ratios have been estimated from the Gibbs energy differences between all the accessible transition states by using the Curtin−Hammet principle.[4]

2. Computational Methodology

Geometry optimizations were performed using the density functional theory (DFT) with the three-parameter hybrid functional B3LYP[5,6] and the 6-31G(d,p) basis set, involving polarized functions on both hydrogens and heavy atoms. A mass of studies demonstrated that this level of theory is suitable for optimizing the geometries of radical systems.[7−11] It was also shown by Méreau et al. that B3LYP/6-31G(d,p) calculations can estimate with a good accuracy the activation energy of alcoxy and carbonyl radicals decomposition and isomerization unimolecular reactions.[12] In the case of transition states, improved single point energies were also calculated within the larger 6-311+G(d,p) basis set, to address the impact of diffuse functions in the relative energies. However, recent studies have shown that B3LYP calculations may lead to underestimations of reaction barriers for radical reactions.[13] In particular, Maxwell and co-workers demonstrated that B3LYP calculations underestimate the free energy difference in 5-*exo* cyclizations of *N*-alkyl-4-pent-4-enylaminyl when comparing to high level CBS-RAD(B3LYP,B3LYP) calculations.[14]

Then, to check the reliability of the computational schemes, single point energies have also been calculated at the BH&HLYP/6-311+G(d,p) level. Indeed, the BH&HLYP functional,[6,15] including 50% Hartree−Fock and 50% Slater exchange, has been shown to be a good compromise for calculating barrier heights among currently available methods.[10,16] Finally, single point calculations were also performed at the restricted open shell second-order Møller−Plesset (ROMP2)[17] level with both the 6-31G(d,p) and 6-311+G(d,p) basis sets, as it was shown by Radom and collaborators that ROMP2 single-point energies on UB3LYP geometries perform well in predicting radical stabilization energies.[18]

Thermochemical quantities are composed of the relative energies calculated at the various levels of theory cited above (determined using the B3LYP/6-31G(d,p) geometries), and of thermal corrections derived from the unscaled B3LYP/6-31G(d,p) harmonic vibrational frequencies. Thermal corrections were calculated using standard temperature and pressure (STP) conditions (298.15 K, 1 bar) for all the compounds, to evaluate the influence of the nature of the allylic substituent on the stereochemistry, as well as using the experimental temperature (e.g., −50 °C for X = $SiMe_3$ and X = OH, and 80 °C for X = *t*-Bu) to compare with the experimentally measured stereoselectivities.

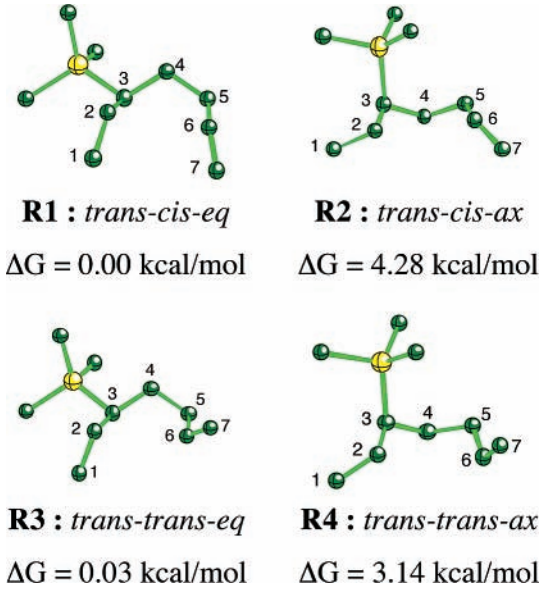

Figure 1. Optimized geometries and relative Gibbs free energies at 298.15 K obtained at the B3LYP/6-31G(d,p) level of the four trans-1,2 activated reactants of radical I with X = $SiMe_3$. Hydrogen atoms are hidden for clarity.

Electronic distribution analyses are performed using Mulliken atomic charges,[19] as well as atomic charges fitted to the electrostatic potential using the CHELPG scheme.[20] The average spin expectation values $\langle S^2 \rangle$ of the transition states range from 0.783 (B3LYP) to 0.826 (BH&HLYP), which suggests no significant error due to spin contamination. All calculations were carried out using Gaussian 03.[21] The geometries (Gaussian Archive Entries), energies and thermal corrections under STP conditions of all stationary points described in the paper are provided as Supporting Information.

3. 5-*exo*-Trig Cyclizations with X = $SiMe_3$

3.1. Activated Reactants. In β-substituted organosilicon radicals, the presence of the bulky silicon group within the chain restricts the number of reactive conformations, favoring an anti configuration of the C2 and C3 centers.[22] We then restricted our study to trans-2,3 structures a priori favorable to cyclization. Moreover, to simplify the reading, the same nomenclature cis/trans was used to indicate the geometrical configuration of cyclized as well as *noncyclized* radicals. The distinct stereomers are then referred relative to their trans/cis C3−C2 and C2−C6 stereochemistry, followed by a mention of the axial (ax) or equatorial (eq) position adopted by the allylic group. The numbering of the carbon atoms corresponds to the one used in the reference paper.[1]

Four distinct reactive structures activated for cyclization were found at the B3LYP/6-31G(d,p) level. The optimized geometries as well as the relative Gibbs free energies under STP are reported in Figure 1.

In the two most stable structures **R1** and **R3**, the carbon C4 lies above the mean C2−C3−C5−C6 plane, on the same side

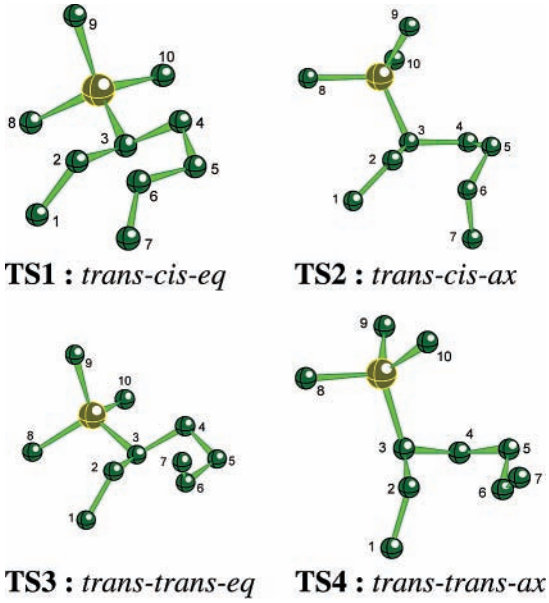

Figure 2. Optimized geometries of the four possible transition structures of radical I with a trans-2,3 stereochemistry and X = $SiMe_3$. Hydrogen atoms are hidden for clarity.

as the silicon group. The distance between C2 and C6 is equal to 3.11 Å (**R1**) and 3.19 Å (**R3**). In the two highest energy structures **R2** and **R4**, C4 is located on the opposite side of the C2−C3−C5−C6 plane with respect to Si, whereas the C2−C6 distance is larger and amounts to 3.37 Å (**R2**) and 3.28 Å (**R4**). In **R1**, the carbon C1 is in the syn position with respect to C7, corresponding to a C3−C2−C6 trans−cis geometry, whereas in **R3** C1 and C7 they are oriented in the anti position, corresponding to a C3−C2−C6 trans−trans geometry.

In **R1** and **R3**, the silicon group adopts a pseudo-equatorial position, whereas it is pseudo-axial in the two highest energy conformers. The pseudo-equatorial position, in which the C2−C6 and the C3−Si axes are close to be aligned, maximizes the stabilization effects due to hyperconjugation from the bonding orbital of the Si−C3 bond into the half-filled hybrid orbital at the radical center.[23] The magnitude of this hyperconjugation effect was evaluated at the B3LYP/6-31G(d,p) level by calculating the rotational barrier around the C−C bond in the β-Si-substituted alkyl radical $H_3SiCH_2CH_2^{\bullet}$ and was found to be 2.46 kcal/mol at 298.15 K, in agreement with previous experimental[24] and ab initio determinations.[25]

The atomic spin densities reported in the Supporting Information show that the free electron at C2 is slightly delocalized on C3 and C1. It is also noticeable that the spin density values on Si is larger, although slightly, in the equatorial than in the axial structures due to hyperconjugation.

3.2. Transition States. Four different transition states with a trans-2,3 stereochemistry have been optimized at the B3LYP/6-31G(d,p) level and are schematized on Figure 2. The relative Gibbs free energies calculated under STP conditions within various levels of theory are listed in Table 1. The corresponding values calculated using the experimental temperature of 223 K are given in the Supporting Information. Each transition state has been characterized by the existence of one single vibrational normal mode associated with an imaginary frequency, corresponding to the relative motion of carbons C2 and C6 related to the formation/breaking of the covalent bond during the cyclization, as illustrated in Figure 3 for **TS1**.

The relative ordering of the four transition states is independent of the temperature and of the level of theory used to

TABLE 1: Relative Gibbs Free Energies (kcal/mol) at 298.15 K for the Four Possible Transition Structures of Radical I with a Trans-2,3 Stereochemistry and X = $SiMe_3$ Obtained within Various Levels of Calculation[a]

	1	2	3	4	5
TS1: trans−cis−eq	0.00	0.00	0.00	0.00	0.00
TS2: trans−cis−ax	4.58	4.17	4.18	4.13	3.43
TS3: trans−trans−eq	0.99	0.85	1.00	1.31	1.05
TS4: trans−trans−ax	3.03	2.93	2.62	3.10	2.52

[a] (1) B3LYP/6-31G(d,p)//B3LYP/6-31G(d,p). (2) B3LYP/6-311+G(d,p)//B3LYP/6-31G(d,p). (3) BH&HLYP/6-311+G(d,p)//B3LYP/6-31G(d,p). (4) ROMP2/6-31G(d,p)//B3LYP/6-31G(d,p). (5) ROMP2/6-311+G(d,p)//B3LYP/6-31G(d,p).

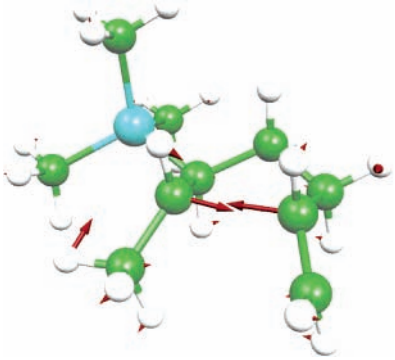

Figure 3. Atomic displacement vectors of the vibrational normal mode associated to the imaginary frequency for the trans−cis−eq transition structure of radical I with X = $SiMe_3$.

determine the electronic wave function. The geometries of the two lowest energy structures are in agreement with the model of Beckwith and Schiesser,[2] further refined by Spellmeyer and Houk.[3] The lowest energy structure **TS1** displays a chairlike geometry in which the carbon C1 is in syn position with respect to C7, corresponding to a C3−C2−C6 trans−cis relative configuration. The minor product is formed through the boatlike **TS3** corresponding to a C3−C2−C6 trans−trans relative configuration. As mentioned by Houk, this structure is higher in energy (by 0.85−1.31 kcal/mol under STP) because of higher torsional strain. A decrease of the temperature from 298.15 to 223 K leads to an increase of 0.25 kcal/mol in the energy difference between **TS1** and **TS3**.

At both the B3LYP and ROMP2 levels, the inclusion of diffuse functions decreases the energy difference between **TS1** and **TS3**, whereas the use of the BH&HLYP functional instead of the B3LYP leads to the opposite effect.

In both **TS1** and **TS3**, a pseudo-equatorial position is adopted preferentially by the silicon group, whereas in the two structures of higher energies, **TS2** and **TS4**, the $SiMe_3$ group is pseudo-axial. The four transition structures are then quite similar to their corresponding reactive forms, with the exception of the much lower distance of 2.23−2.25 Å between the carbons C2 and C6 involved in the cyclization, in agreement with recent ab initio calculations of Tripp et al.[26] related to cyclizations of hexenyl radicals substituted by bulky groups. The bond length C6−C7 amounts to 1.37 Å in every TS, which corresponds to a very small increase compared to those in reactants, in agreement with the picture of an early transition state.

The atomic charge analysis (Table 2) does not reveal significant differences compared to the cases of the reactants. The Me groups attached to Si as well as C3 carry a large excess of electrons, as a consequence of the σ-donor character of Si, charged positively. The charge on the carbon C2 calculated within the ChelpG scheme is significantly positive, which

TABLE 2: B3LYP/6-31G(d,p) Mulliken and ChelpG Atomic Charges for the Four Possible Transition Structures of Radical I with a Trans-2,3 Stereochemistry and X = $SiMe_3$[a]

	TS1: trans−cis−eq		TS2: trans−cis−ax		TS3: trans−trans−eq		TS4: trans−trans−ax	
	Mulliken	CHelpG	Mulliken	CHelpG	Mulliken	CHelpG	Mulliken	CHelpG
Si	0.753	0.557	0.753	0.584	0.754	0.545	0.755	0.640
C1	−0.317	−0.262	−0.328	−0.316	−0.333	−0.305	−0.332	−0.268
C2	−0.079	0.176	−0.079	0.227	−0.075	0.186	−0.081	0.171
C3	−0.241	−0.150	−0.240	−0.197	−0.246	−0.150	−0.248	−0.216
C4	−0.191	−0.023	−0.189	0.123	−0.179	0.067	−0.189	0.015
C5	−0.195	0.002	−0.194	−0.054	−0.204	−0.031	−0.196	−0.026
C6	−0.048	0.091	−0.069	0.075	−0.054	0.067	−0.037	0.063
C7	−0.246	−0.443	−0.237	−0.437	−0.246	−0.447	−0.253	−0.426

[a] See Figure 1 for the atom labels.

TABLE 3: B3LYP/6-31G(d,p) Mulliken Atomic Spin Densities in the Two Lowest Energy Transition Structures of Radical I with X = $SiMe_3$[a]

	TS1: trans−cis−eq	TS3: trans−trans−eq
Si	0.043	0.045
C2	0.649	0.650
C6	−0.226	−0.230
C7	0.592	0.577

[a] See Figure 1 for the atom labels.

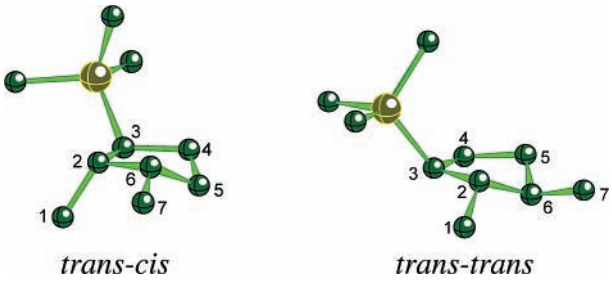

Figure 4. Optimized geometries of the two cyclized structures of radical I with a trans-2,3 stereochemistry and X = $SiMe_3$. Hydrogen atoms are hidden for clarity.

corroborates the assumption made by James et al. about the stabilization of an electron deficiency on the radical center C2 due to the presence of the β-silicon group. This effect is still present regarding the Mulliken distribution, although less pronounced: the radical center C2 is close to neutrality, whereas the other carbons along the chain all carry significant negative charges. The spin density values carried by the three reactive centers C2, C6, C7 and by Si, reported in Table 3 for **TS1** and **TS3**, indicate that the free electron is mainly delocalized between C2 and C7 according to simple mesomery. The spin density carried out by the silicon atom decreases compared to those for the reactants due to the radical migration toward C7.

3.3. Cyclized Products. Although four reactive and four transition structures have been located, only two distinct cyclized products were revealed by quantum calculations. IRC (intrinsic reaction coordinate) procedures carried out at the lower B3LYP/6-31G level demonstrated that both **TS1** and **TS2** provide the same trans−cis isomer, whereas both **TS3** and **TS4** lead to the trans−trans (see Figure 4).

At the ROMP2/6-311+G(d,p)//B3LYP/6-31G(d,p) level, the trans−cis structure, corresponding experimentally to the major product, is 1.75 kcal/mol higher in energy than the trans−trans. In the trans−cis stereomer, the carbons C2−C3−C4−C6 are quasi coplanar. The carbon C5 is out of the base plane and on the same side as carbons C1 and C7. In the trans−trans stereomer, the base plane is composed of the C2, C3, C4 and C5 atoms, whereas the substituted carbon C6 is significantly located out of the plane. In both structures, the $SiMe_3$ group is

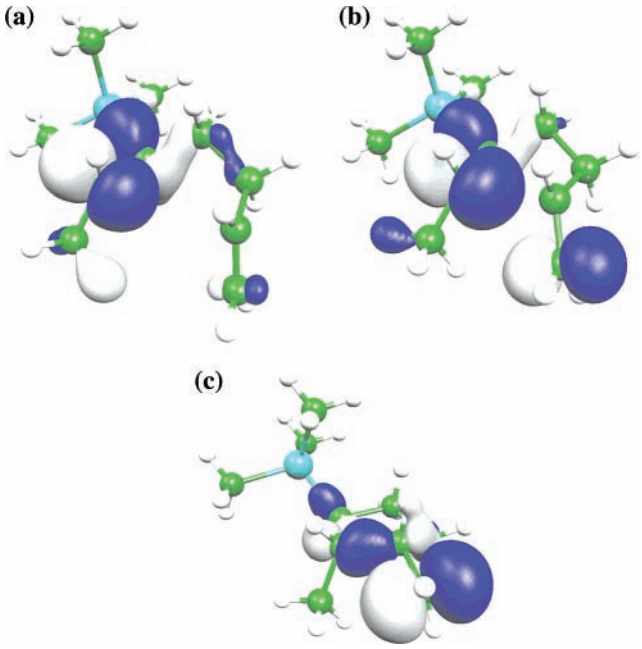

Figure 5. Singly occupied molecular orbital for the reactive (a), transition (b) and cyclized (c) structures of radical I with X = $SiMe_3$ obtained at the ROHF/6-31G(d,p) level.

located 52−54° above the base plane, which corresponds to an intermediate location between an axial and equatorial position. The change in the position of the $SiMe_3$ group when going from the TS to the products, and therefore the existence of only two cyclized isomers instead of four, may be rationalized as a consequence of the loss of hyperconjugation effects due to the radical migration during the cyclization. This migration is illustrated in Figure 5 by the changes in the localization of the singly occupied molecular orbital (SOMO) during the cyclization process. In both cyclized isomers, the spin density on Si is not significant, and the free electron is mainly localized in C7 carbon. A small delocalization of the radical on C6 and C2 is nevertheless observed.

3.4. Estimation of the Product Ratios. The energy diagram of the cyclization process is schematized Figure 6. The free energy differences ΔG_i^0 between the reactive conformational isomers are more than one order of magnitude smaller than the activation energies for the formation of the products. Assuming that the various reactive conformers are in rapid equilibrium relative to the rate of product formation, and that this interconversion equilibrium is maintained throughout the reaction, the Curtin−Hammet principle[4] may be applied, which states that the product ratios are controlled only by the differences in the standard Gibbs free energies ΔG_i of the accessible transition states. For a number N of contributing conformations, the

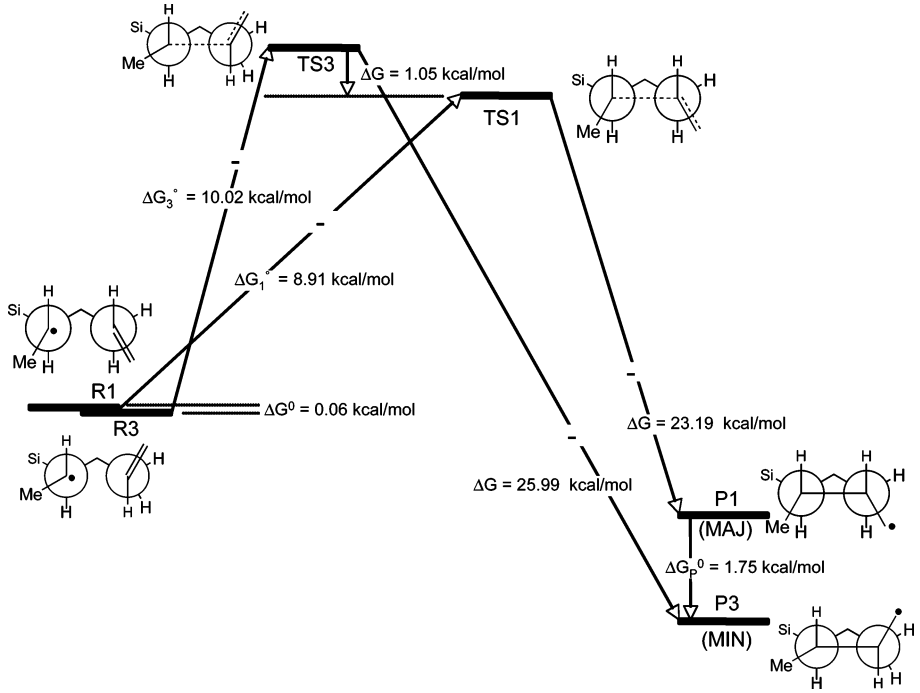

Figure 6. Energy diagram for the cyclization of radical I with the $SiMe_3$ group in the allylic position. The reported free energy values have been calculated at the ROMP2/6-311+G(d,p)//B3LYP/6-31G(d,p) level under STP conditions.

TABLE 4: Trans−Cis:Trans−Trans Relative Populations of Cyclized Stereomers III with X = $SiMe_3$

	298.15 K	223 K
B3LYP/6-31G(d,p)//B3LYP/6-31G(d,p)	84:16	94:6
B3LYP/6-311+G(d,p)//B3LYP/6-31G(d,p)	80:20	92:8
BH&HLYP/6-311+G(d,p)//B3LYP/6-31G(d,p)	84:16	94:6
ROMP2/6-31G(d,p)//B3LYP/6-31G(d,p)	90:10	97:3
ROMP2/6-311+G(d,p)//B3LYP/6-31G(d,p)	84:16	95:5
exp[a] (223 K)		>99:<1

[a] See ref 1.

relative population (P_i) of product i connected to the ith transition state will then be given by performing a simple Maxwell−Boltzmann statistics over all the possible TS:

$$P_i = \frac{\exp(-\Delta G_i/RT)}{\sum_{i=1}^{N}\exp(-\Delta G_i/RT)}$$

These ratios have been estimated at both the standard and the experimental temperatures using the relative Gibbs free energies ΔG_i reported in Table 1 and in the Supporting Information. In the latter case, the theoretical values are compared in Table 4 with the experimental ratios issued from ^{1}H NMR and GC analysis of the crude reaction mixture.[1] As it was shown that two TS displaying the same 2,6-stereochemistry lead to the same product independently of the axial or equatorial position of the silicon group, the relative populations of the trans−trans−ax and trans−trans−eq structures have been summed to obtain the ratio of the trans−trans-substituted cyclopentane, and similarly for the trans−cis.

As expected, the cyclization process is more selective at lower temperature. All levels of calculation reproduce fairly well the experimentally measured selectivities at $T = 223$ K. DFT results do not depend significantly on the functional and basis set. Compared to ROMP2 calculations, DFT calculations overestimate slightly the population of the minor product.

TABLE 5: Relative Gibbs Free Energies (kcal/mol) at 298.15 K for the Eight Possible Transition Structures of Radical I with X = *t*-Bu Obtained within Various Levels of Calculation[a]

	1	2	3	4	5
cis−cis−eq	4.19	4.06	4.12	3.61	3.29
cis−cis−ax	8.39	8.31	8.45	8.37	7.66
cis−trans−eq	2.95	2.81	2.77	2.71	2.27
cis−trans−ax	9.44	9.18	9.40	9.52	8.73
trans−cis−eq	0.00	0.00	0.00	0.00	0.00
trans−cis−ax	3.97	3.66	3.81	3.77	3.24
trans−trans−eq	1.55	1.41	1.51	1.67	1.40
trans−trans−ax	2.34	2.10	2.17	2.51	2.10

[a] (1) B3LYP/6-31G(d,p)//B3LYP/6-31G(d,p). (2) B3LYP/6-311+G(d,p)//B3LYP/6-31G(d,p). (3) BH&HLYP/6-311+G(d,p)//B3LYP/6-31G(d,p). (4) ROMP2/6-31G(d,p)//B3LYP/6-31G(d,p). (5) ROMP2/6-311+G(d,p)//B3LYP/6-31G(d,p).

4. 5-*exo*-Trig Cyclizations with X = *t*-Bu

To size up the magnitude of steric effects due to the bulky β-substituent, we did not a priori assume any preferential stereochemical conformation of the C2 and C3 centers, contrary to the silylated series. Besides, because product ratios are controlled by the free energies differences between the accessible transition states (see discussion above), we do not treat in this part of activated reactants. The full set of possible transition states, including the cis-2,3 stereomers, has then been optimized at the B3LYP/6-31G(d,p) level, and relative Gibbs free energies are listed in Table 5.

All levels of calculation provide the same hierarchy in the relative energies of the different TS. Not surprisingly, the structures displaying a cis-2,3 conformation are more than 2.2 kcal/mol higher in energy than the ones displaying a trans-2,3 stereochemistry and constitute therefore inaccessible ways toward the products. The trans−cis−eq structure is the lowest in energy, giving rise mainly to the trans−cis cyclized stereomer. Similarly to $SiMe_3$, equatorial positions are preferentially adopted by the alkyl group in the TS (see Figure 7). The minor product is formed through the trans−trans−eq TS, which is

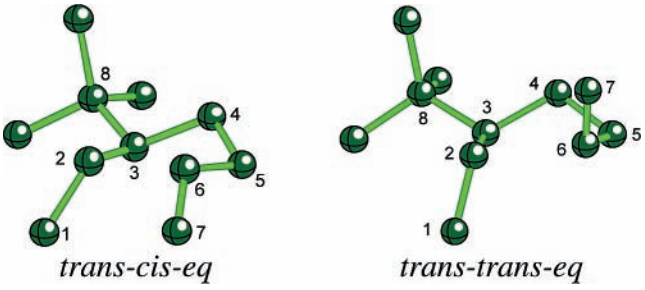

Figure 7. Optimized geometries of the two lowest energy transition structures of radical I with X = *t*-Bu. Hydrogen atoms are hidden for clarity.

TABLE 6: Relative Gibbs Free Energies at 298.15 K (kcal/mol) for the Eight Possible Cyclized Structures of Radical I with X = *t*-Bu Obtained at the B3LYP/6-31G(d,p) Level

	ΔG_{298}
cis−cis−eq	4.26
cis−cis−ax	10.00
cis−trans−eq	4.24
cis−trans−ax	5.65
trans−cis	2.66
trans−trans (1)	0.83
trans−trans (2)	0.00

higher in energy by 1.40−1.67 kcal/mol at room temperature. This energy difference is similar to that under the experimental temperature of 353 K (see Supporting Information). Within both DFT and ROMP2 methods, the use of the diffuse 6-311+G(d,p) basis set instead of 6-31G(d,p) decreases the energy difference between the trans−cis−eq and the trans−trans−eq structures.

The optimized geometries are globally similar to those obtained with X = Si, with the exception of the C3−C8 bond (1.58 Å), which is much shorter than the C3−Si bond (1.92−1.95 Å). The analysis of the CHelpG atomic charges reveals that the electron deficiency on the radical center C2 is similar to that obtained with the silylated substituent. The spin density on C8 is twice smaller than the one obtained on Si in the equivalent structures, indicating that stabilization effects due to the free radical delocalization on the β-substituent should be of smaller magnitude.

The most stable cyclized structures corresponds to the two trans−trans cyclopentanes, differing by 0.83 kcal/mol at the B3LYP/6-31G(d,p) level (Table 6). These two structures differ by the carbon atoms defining the base plane of the pentacycle, C2−C3−C4−C5 in the former, and C2−C3−C4−C6 in the latter (see Figure 8). The *t*-Bu group is located around 50° above the base plane. The trans−cis structure, corresponding to the major product, is higher in energy by 2.66 kcal/mol. In this structure the position of the *t*-Bu group is 67° above the base plane. In structures displaying a cis-2,3 stereochemistry, higher in energy, the *t*-Bu is stabilized in either the equatorial or axial position.

The relative populations of cyclized diastereomers estimated by using the relative TS energies are reported in Table 7 (as in the previous section, the relative populations of two products displaying the same 2,3 stereochemistry are summed). As in the case of silylated radicals, all levels of theory predict a similar trans−cis:trans−trans ratio. At T = 353 K, the theoretical selectivities are in very good adequacy with the experimental ones.

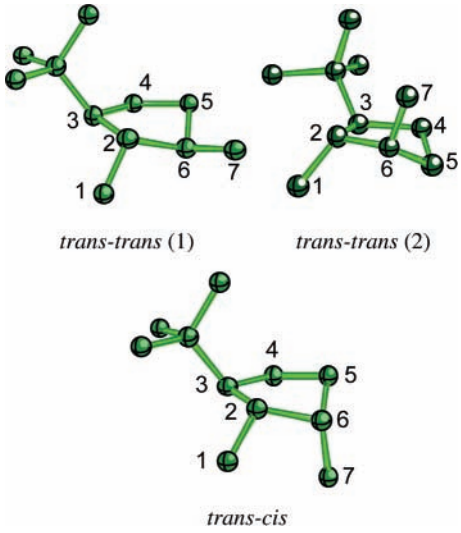

Figure 8. Optimized geometries of the three lowest energy cyclized structures of radical I with X = *t*-Bu. Hydrogen atoms are hidden for clarity.

TABLE 7: Relative Populations[a] of Cyclized Products with X = *t*-Bu

	298 K	353 K
B3LYP/6-31G(d,p)//B3LYP/6-31G(d,p)	0:1:91:8	0:1:86:13
B3LYP/6-311+G(d,p)//B3LYP/6-31G(d,p)	0:1:88:11	0:1:82:17
BH&HLYP/6-311+G(d,p)//B3LYP/6-31G(d,p)	0:1:90:9	0:2:84:14
ROMP2/6-31G(d,p)//B3LYP/6-31G(d,p)	0:1:92:7	0:2:87:11
ROMP2/6-311+G(d,p)//B3LYP/6-31G(d,p)	1:2:87:11	0:3:81:16
exp[b] (353 K)		0:0:100:0

[a] Given following the order: cis−cis:cis−trans:trans−cis:trans−trans. [b] See ref 1.

5. 5-*exo*-Trig Cyclizations with X = OH

5.1. Activated Reactants. Geometry optimizations of the whole set of the reactive forms of the radical **I** with an hydroxy group in allylic position were carried out at the B3LYP/6-31G(d,p) level. All structures and relative energies are available in the Supporting Information. As a consequence of the small size of the allylic hydroxy group and the absence of large steric effects, the structures with either a cis- or a trans-2,3 stereochemistry are very close in energy. The free energies of all the reactants are separated by less than 0.73 kcal/mol. All structures adopt either a chairlike or a boatlike geometry in which the carbons C2, C3, C5 and C6 are quasi coplanar. The distance between the two reactive centers C2 and C6 ranges from 3.17 Å (cis−trans−eq) to 3.25 Å (cis−cis−eq).

5.2. Transition States. The structures of the eight possible transition species optimized at the B3LYP/6-31G(d,p) level are schematized in Figure 9 and their relative Gibbs free energies calculated at 298.15 K are given Table 8. The corresponding values obtained at 223 K are reported in the Supporting Information.

Except for the B3LYP/6-311+G(d,p)//B3LYP/6-31G(d,p) level, all DFT calculations predict the all-cis structure with OH in the axial position as the lowest in energy, followed by the trans−cis−eq and the trans−trans−ax structures. The hierarchy between the energies of the two latter stereomers is reversed at the MP2 level. In all structures the distance between C2 and C6 ranges between 2.24 and 2.26 Å. The three highest structures in energy adopt boatlike geometries in which OH is in the equatorial position, and at least one of the substituent in C1 or C7 lies on the same side of the C2−C3−C5−C6 plane as C4, leading to high torsional strain.

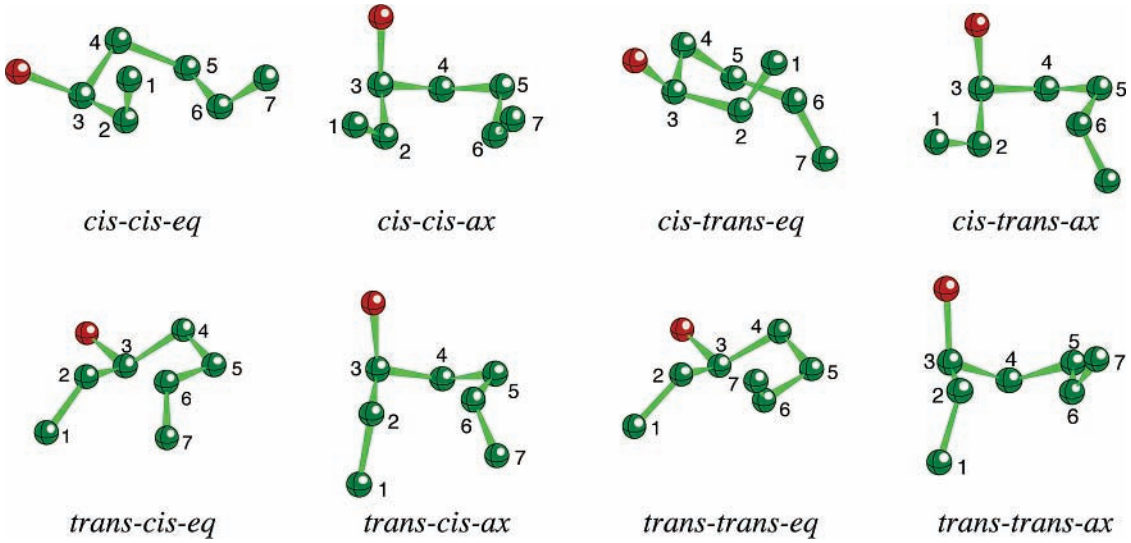

Figure 9. Optimized geometries of the transition structures of radical I with X = OH. Hydrogen atoms are hidden for clarity.

TABLE 8: Relative Gibbs Free Energies (kcal/mol) at 298.15 K for the Eight Possible Transition Structures of Radical I with X = OH[a]

	1	2	3	4	5
cis−cis−eq	3.12	2.81	2.85	3.04	2.31
cis−cis−ax	0.00	0.15	0.00	0.00	0.00
cis−trans−eq	1.58	1.29	1.30	1.93	1.19
cis−trans−ax	1.10	1.10	1.07	1.24	1.11
trans−cis−eq	0.50	0.00	0.06	1.00	0.34
trans−cis−ax	1.41	1.10	1.08	1.25	0.70
trans−trans−eq	2.00	1.41	1.63	2.63	1.79
trans−trans−ax	0.54	0.28	0.25	0.77	0.16

[a] (1) B3LYP/6-31G(d,p)//B3LYP/6-31G(d,p). (2) B3LYP/6-311+G(d,p)//B3LYP/6-31G(d,p). (3) BH&HLYP/6-311+G(d,p)//B3LYP/6-31G(d,p). (4) ROMP2/6-31G(d,p)//B3LYP/6-31G(d,p). (5) ROMP2/6-311+G(d,p)//B3LYP/6-31G(d,p).

TABLE 9: Relative Gibbs Free Energies at 298.15 K (kcal/mol) for the Eight Possible Cyclized Structures of Radical I with X = OH

	ΔG_{298}
cis−cis−eq	3.22
cis−cis−ax	3.28
cis−trans−eq	0.00
cis−trans−ax	0.30
trans−cis−eq	2.16
trans−cis−ax	2.27
trans−trans−eq	0.09
trans−trans−ax	/

The spin density on the oxygen atom in the equatorial structures is about 0.015, i.e., three times smaller than that obtained in the corresponding transition species with X = $SiMe_3$. The spin density value on O in the *axial* structures is zero.

5.3. Cyclized Products and Stereoselectivities. The relative Gibbs free energies of cyclized forms of radical **I** under STP obtained at the B3LYP/6-31G(d,p) are reported in Table 9. The lowest energy is obtained for the *cis*−trans−eq stereomer, corresponding to the minor experimental product. The all-cis cyclopentane, corresponding to the major product, is associated with an energy higher by 3.2 kcal/mol at 298.15 K. The theoretical ratios of cyclized cyclopentanes are reported in Table 10.

In every cases, the stereocontrol is less efficient than that observed with the bulky $SiMe_3$ or *t*-Bu groups, the range of energy difference between the TS being reduced. In agreement with experiments, the major product corresponds to the cis−cis conformer using levels of calculation 1, 4 and 5. The population of the trans−cis stereomer, corresponding to the minor product observed experimentally, is overestimated by levels 2 and 3. Finally, all levels of theory predict the formation of the trans−trans product, not observed experimentally, in similar proportion to the minor product.

The cis-selective cyclization of the hydroxy substituted radical is not in line with the Beckwith−Houk model. Favorable electronic effects were invoked in previous studies[27] to rationalize the axial position preferentially adopted by the alcohol group. The axial OH group being orthogonal to the electron-deficient forming C2−C6 bond, the charge at C2 would be better stabilized by the C3−H bond nearly aligned to C2−C6, as a σ_{C-H} bond is a better electron-donor than a σ_{C-O} bond. However, the comparison of the ChelpG electronic distributions between the cis−cis−ax and cis−cis−eq transition structures does not allow confirmation of this hypothesis. Indeed, the partial charge at the radical center C2 is smaller in the cis−cis−ax conformer (0.076e) than in the cis−cis−eq (0.210e). The Mulliken atomic charge at C2 is nevertheless slightly *less negative* in cis−cis−ax than in cis−cis−eq.

As illustrated in Figure 10, the slight stabilization of the cis−cis−ax transition state might arise from the presence of three equivalent electrostatically favorable long-range O−H interactions. Only two of these interactions are present in the trans−cis−eq transition state, giving rise to the minor product. This type of stabilization, involving the presence of a pseudo-five-membered intramolecular cycle, was previously invoked to explain the relative population of rotamers of dimethyl-L-tartrate conformers.[28] Note that the same pattern also exists in the cis−trans−ax conformer, higher in energy by 1 kcal/mol because of higher torsional strain.

6. Conclusions

In complement to the experimental work of James et al., the stereochemistry of free radical mediated 5-*exo*-trig cyclizations incorporating various allylic substituents has been studied by using ab initio approaches. The reactive, transition and cyclized structures of radical **I** have been fully analyzed in terms of structural parameters, energies and electronic distributions.

5-*exo*-trig cyclizations incorporating bulky silylated or *t*-Bu agree with the Beckwith−Houk models: the major product is formed through a chairlike TS with a 2,6-cis stereochemistry. In the transition structures, steric effects favor the equatorial

TABLE 10: Relative Populations[a] of Cyclized Products with X = OH

	298.15 K	223 K
(1) B3LYP/6-31G(d,p)//B3LYP/6-31G(d,p)	46:10:24:20	59:5:18:18
(2) B3LYP/6-311+G(d,p)//B3LYP/6-31G(d,p)	27:9:40:24	31:5:40:24
(3) BH&HLYP/6-311+G(d,p)//B3LYP/6-31G(d,p)	33:9:35:24	40:5:32:23
(4) ROMP2/6-31G(d,p)//B3LYP/6-31G(d,p)	57:9:17:16	73:4:10:13
(5) ROMP2/6-311+G(d,p)//B3LYP/6-31G(d,p)	34:10:29:27	42:5:23:29
exp[b] (223 K)		70:0:30:0

[a] Given following the order: cis−cis:cis−trans:trans−cis:trans−trans. [b] See ref 1.

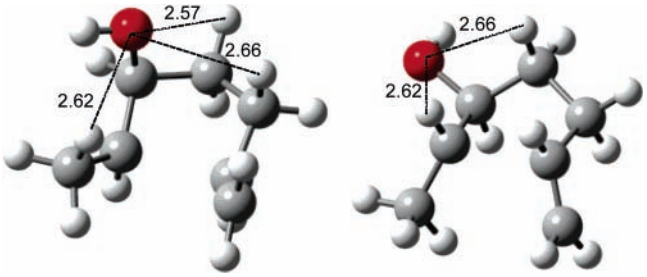

Figure 10. Electrostatically favorable long-range O−H interactions in the two lowest energy transition states (distances in Å).

position of the silicon group. The product ratio estimated from calculations predict a very high level of stereocontrol, in agreement with experiments. In accordance with experimental results, precursors bearing an hydroxy group have been shown to provide the cis−cis stereochemistry, whereas the minor product corresponds to the trans−cis stereomer. These results are not described by the Beckwith−Houk model.

To summarize, the stereocontrol of radical 5-*exo*-trig cyclizations implying allylic $SiMe_3$, *t*-Bu or OH groups may be rationalized following simple rules acting on transition structures.

(i) The most stable TS adopts one of the pseudo chair conformations:

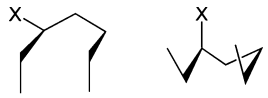

(ii) Bulky X groups favor the trans−cis−eq conformation with a very high level of stereocontrol due to steric effects

(iii) For small X groups, the level of stereocontrol is lower and the stereochemistry of the major stereomer is mainly driven by electronic effects. When a hydroxy group is involved, the cis−cis−ax configuration is slightly stabilized compared to the trans−cis−eq configuration, possibly due to the presence of long-range electrostatic O−H interactions.

Acknowledgment. Ph.d'A. thanks the European Community for his doctoral Marie Curie Fellowship. Ph.d'A. is also grateful to the Belgian Government (IUAP no. P5-03 "Supramolecular Chemistry and Supramolecular Catalysis") and the F.R.I.A. ("Fonds pour la Formation à la Recherche dans l'Industrie et dans l'Agriculture") for financial support in the frame of his Ph.D. Ph.d'A. and F.C. thank Professor D. Liotard, Dr. R. Méreau and Dr. B. Champagne for fruitful discussions. The calculations were performed thanks to computing time made available by the "SiMoA" (Simulation et Modélisation en Aquitaine, France), the intensive calculation pole "M3PEC-MESOCENTRE" of the University Bordeaux I, the "IDRIS" (Institut du Développement et des Ressources en Informatique Scientifique, France, project 51836) and the Interuniversity Scientific Computing Facility (ISCF), installed at the Facultés Universitaires Notre-Dame de la Paix (Namur, Belgium), for which Ph.d'A. gratefully acknowledges the financial support of the FNRS-FRFC and the "Loterie Nationale" for the convention no. 2.4578.02 and of the FUNDP. P.J. and Y.L. gratefully acknowledge the *Ministère de la Recherche et de la Technologie* for a Ph.D. grant and the *Institut Universitaire de France* and the CNRS for financial support.

Supporting Information Available: Energies and structures of all stationary points described in the paper. This material is available free of charge via the Internet at http://pubs.acs.org.

References and Notes

(1) (a) James, P.; Landais, Y. *Org. Lett.* **2004**, *6*, 325. (b) James, P.; Felpin, F.-X.; Landais, Y.; Schenk, K. *J. Org. Chem.* **2005**, *70*, 7985.

(2) (a) Beckwith, A. L. J.; Schiesser, C. H. *Tetrahedron Lett.* **1985**, *26*, 373. (b) Beckwith, A. L. J.; Schiesser, C. H. *Tetrahedron* **1985**, *41*, 3925. (c) Beckwith, A. L. J.; Zimmermann, J. *J. Org. Chem.* **1991**, *56*, 5791.

(3) Spellmeyer, D. C.; Houk, K. N. *J. Org. Chem.* **1987**, *52*, 959.

(4) (a) Curtin, D. Y. *Rec. Chem. Prog.* **1954**, *15*, 111. (b) Seeman, J. I. *Chem. Rev.* **1983**, *83*, 83.

(5) Becke, A. D. *J. Chem. Phys.* **1993**, *98*, 5648.

(6) Lee, C.; Yang, W.; Parr, R. G. *Phys. Rev. B* **1988**, *37*, 785.

(7) Zipse, H. *J. Am. Chem. Soc.* **1997**, *119*, 2889.

(8) Mohr, M.; Zipse, H.; Marx, D.; Parrinello, M. *J. Phys. Chem. A* **1997**, *101*, 8942.

(9) Newcomb, M.; Horner, J. H.; Whitted, P. O.; Crich, D.; Huang, X.; Yao, Q.; Zipse, H. *J. Am. Chem. Soc.* **1999**, *121*, 10685.

(10) Wang, Y.; Grimme, S.; Zipse, H. *J. Phys. Chem. A* **2004**, *108*, 2324.

(11) Gomez-Balderas, R.; Coote, M. L.; Henry, D. J.; Radom, L. *J. Phys. Chem. A* **2004**, *108*, 2874.

(12) (a) Méreau, R.; Rayez, M. T.; Caralp, F.; Rayez, J. C. *Phys. Chem. Chem. Phys.* **2000**, *2*, 1919. (b) Méreau, R.; Rayez, M. T.; Caralp, F.; Rayez, J. C. *Phys. Chem. Chem. Phys.* **2000**, *2*, 3765. (c) Méreau, R.; Rayez, M. T.; Caralp, F.; Lesclaux, R. *Phys. Chem. Chem. Phys.* **2001**, *3*, 4712. (d) Méreau, R.; Rayez, M. T.; Caralp, F.; Rayez, J. C. *Phys. Chem. Chem. Phys.* **2003**, *5*, 4828. (e) Caralp, F.; Devolder, P.; Fittschen, C.; Gomez, N.; Hippler, H.; Méreau, R.; Rayez, M. T.; Striebel, F.; Viskolcz, B. *Phys. Chem. Chem. Phys.* **1999**, *1*, 2935.

(13) (a) Lynch, B. J.; Fast, P. L.; Harris, M.; Truhlar, D. G. *J. Phys. Chem. A* **2000**, *104*, 4811. (b) Lynch, B. J.; Truhlar, D. G. *J. Phys. Chem. A* **2001**, *105*, 2936.

(14) Maxwell, B. J.; Smith, B. J.; Tsanaktsidis, J. *J. Chem. Soc., Perkin Trans.* **2000**, *2*, 425.

(15) Becke, A. D. *J. Chem. Phys.* **1993**, *98*, 1372.

(16) Durant, J. L. *Chem. Phys. Lett.* **1996**, *256*, 595.

(17) Møller, C.; Plesset, M. S. *J. Chem. Phys.* **1934**, *46*, 618.

(18) (a) Parkinson, C. J.; Mayer, P. M.; Radom, L. *Theor. Chem. Acc.* **1999**, *102*, 92. (b) Parkinson, C. J.; Mayer, P. M.; Radom, L. *J. Chem. Soc., Perkin Trans. 2* **1999**, *11*, 2305.

(19) Mulliken, R. S. *J. Chem. Phys.* **1955**, *23*, 1833.

(20) Breneman, C. M.; Wiberg, K. B. *J. Comput. Chem.* **1990**, *11*, 361.

(21) Frisch, M. J.; Trucks, G. W.; Schlegel, H. B.; Scuseria, G. E.; Robb, M. A.; Cheeseman, J. R.; Montgomery, J. A., Jr.; Vreven, T.; Kudin, K. N.; Burant, J. C.; Millam, J. M.; Iyengar, S. S.; Tomasi, J.; Barone, V.; Mennucci, B.; Cossi, M.; Scalmani, G.; Rega, N.; Petersson, G. A.; Nakatsuji, H.; Hada, M.; Ehara, M.; Toyota, K.; Fukuda, R.; Hasegawa, J.; Ishida, M.; Nakajima, T.; Honda, Y.; Kitao, O.; Nakai, H.; Klene, M.; Li, X.; Knox, J. E.; Hratchian, H. P.; Cross, J. B.; Adamo, C.; Jaramillo, J.; Gomperts, R.; Stratmann, R. E.; Yazyev, O.; Austin, A. J.; Cammi, R.; Pomelli, C.; Ochterski, J. W.; Ayala, P. Y.; Morokuma, K.; Voth, G. A.; Salvador, P.; Dannenberg, J. J.; Zakrzewski, V. G.; Dapprich, S.; Daniels, A. D.; Strain, M. C.; Farkas, O.; Malick, D. K.; Rabuck, A. D.; Raghavachari, K.; Foresman, J. B.; Ortiz, J. V.; Cui, Q.; Baboul, A. G.;

Clifford, S.; Cioslowski, J.; Stefanov, B. B.; Liu, G.; Liashenko, A.; Piskorz, P.; Komaromi, I.; Martin, R. L.; Fox, D. J.; Keith, T.; Al-Laham, M. A.; Peng, C. Y.; Nanayakkara, A.; Challacombe, M.; Gill, P. M. W.; Johnson, B.; Chen, W.; Wong, M. W.; Gonzalez, C.; Pople, J. A. *Gaussian 03*, revision B.04; Gaussian, Inc.: Pittsburgh, PA, 2003.

(22) (a) Fleming, I.; Dunoguès, R.; Smithers, R. *Org. React.* **1989**, *37*, 57. (b) Fleming, I.; Barbero, A.; Walter, D. *Chem. Rev.* **1997**, *97*, 2063. (c) Masse, C. E.; Panek, J. S. *Chem. Rev.* **1995**, *95*, 1293. (d) Fleming, I. *J. Chem. Soc., Perkin Trans. 1* **1992**, 3363. (e) Chabaud, L.; James, P.; Landais, Y. *Eur. J. Org. Chem.* **2004**, 3173.

(23) Apeloig, Y.; Karni, M. Theoretical Aspects and Quantum Mechanical Calculations of Silaaromatic Compounds. In *The Chemistry of Organic Silicon Compounds*; Rappoport, Z., Apeloig, Y., Eds.; Wiley: Chichester, U.K., 1998; Vol. 2, Part 1, 1.

(24) (a) Krusic, P. J.; Kochi, J. K. *J. Am. Chem. Soc.* **1971**, *93*, 846. (b) Kawamura, T.; Kochi, J. K. *J. Am. Chem. Soc.* **1972**, *94*, 648. (c) Griller, D.; Ingold, K. U. *J. Am. Chem. Soc.* **1973**, *95*, 6459. (d) Griller, D.; Ingold, K. U. *J. Am. Chem. Soc.* **1974**, *96*, 6715. (e) Jackson, R. A.; Ingold, K. U.; Griller, D.; Nazran, A. S. *J. Am. Chem. Soc.* **1985**, *107*, 208. (f) Auner, N.; Walsh, R.; Westrup, J. *J. Chem. Soc. Chem. Commun.* **1986**, 207. (g) Wilt, J. W.; Lusztyk, J.; Peeran, M.; Ingold, K. U. *J. Am. Chem. Soc.* **1988**, *110*, 281.

(25) (a) Bernardi, F.; Bottoni, A.; Fossey, J.; Sorba, J. *Tetrahedron* **1986**, *42*, 5567. (b) Bertrand, M. P.; De Riggi, I.; Lesueur, C.; Gastaldi, S.; Nouguier, R.; Jaime, C.; Virgili, A. *J. Org. Chem.* **1995**, *60*, 6040.

(26) Tripp, J. C.; Schiesser, C. H.; Curran, D. P. *J. Am. Chem. Soc.* **2005**, *127*, 5518.

(27) (a) Guindon, Y.; Yoakim, V.; Gorys, V.; Ogilvie, W. W.; Delorme, D.; Renaud, G.; Robinson, J.-F.; Lavallée, A.; Slassi, G.; Jung, J.; Rancourt, K.; Durkin, D.; Liotta, D. *J. Org. Chem.* **1994**, *59*, 1166. (b) Durkin, K.; Liotta, D.; Rancourt, J.-F.; Lavallée, L.; Boisvert, L.; Guindon, Y. *J. Am. Chem. Soc.* **1992**, *114*, 4912.

(28) Buffeteau, T.; Ducasse, L.; Brizard, A.; Huc, I.; Oda, R. *J. Phys. Chem. A* **2004**, *108*, 4080.